Available online at www.sciencedirect.com
SCIENCE DIRECT®
Applied Catalysis A: General 272 (2004) 69–78
APPLIED CATALYSIS A: GENERAL
www.elsevier.com/locate/apcata

Butane dehydrogenation on vanadium supported catalysts under oxygen free atmosphere

M. Volpe [a,*], G. Tonetto [b], H. de Lasa [b]

[a] *Chemical Engineering Department, PLAPIQUI-(UNS-CONICET), Camino La Carrindanga Km 7, CC 717 (8000) Bahía Blanca, Argentina*
[b] *Chemical Reactor Engineering Centre, Faculty of Engineering Science, University of Western Ontario, London, Ont., Canada N6A 5B9*

Received in revised form 7 May 2004; accepted 9 May 2004

Available online 24 June 2004

Abstract

The present study investigates the catalytic *n*-butane dehydrogenation under oxygen free atmosphere using VO_x supported on USY, NaY, γ-Al_2O_3 and α-Al_2O_3. Experiments are developed at 520 °C in a fixed bed microreactor. Catalyst characterization via TPR demonstrates the presence of different VO_x species with the nature of these species being a function of the catalyst support. The acidic properties of the prepared catalysts are also evaluated using NH_3 TPD with the following order of acidity being observed: VO_x/γ-Al_2O_3 > VO_xM/α-Al_2O_3 > VO_x/USY. Reactivity experiments show that the VO_x/USY provides both the highest catalytic activity and butane selectivity, with the VO_x/γ-Al_2O_3 displaying a lower activity and butane selectivity and the other tested catalyst samples being essentially inactive. The superior performance of the VO_x/USY catalyst is assigned to its mild acidity.

Keywords: *n*-Butane; VO_x; USY; Dehydrogenation

1. Introduction

Dehydrogenation of light alkanes in oxygen free atmospheres is a valuable approach to produce alkenes from feedstocks of low-cost saturated hydrocarbons. While supported chromium oxide and supported Pt are typically used as catalysts to perform this reaction in commercial processes [1,2], only few studies have been carried out using vanadium-containing catalysts [3–6].

Important drawbacks still exist with the implementation of this catalytic reaction. First, alkane dehydrogenation is an endothermic process, and it requires relatively high temperatures and low pressures to yields significant fractions of alkenes. Under these conditions, thermal cracking to lighter alkanes and coke formation are also promoted with the alkane transformation being quite unselective given all C−H and C−C bonds display close reactivity. As a reference, an industrial based Pt catalyst 0.1Pt–Zn silicate/Al_2O_3 (Philips STAR) at a 538 °C displays a conversion of 29.8% and a selectivity to olefins of 76.4%.

Notwithstanding the strong influence of the support on the physicochemical nature of VO_x species, it appears that one of the key variables in controlling the performance of VO_x catalysts is the nature of the oxide carrier. In this context, the purpose of this work is to determine the activity and selectivity of supported vanadium on four different materials: γ-Al_2O_3 and α-Al_2O_3, USY (ultrastable HY) and NaY zeolite.

Both, γ-alumina and USY zeolite are solid acids. It is thus expected that alkane dehydrogenation using these supports will be accompanied with undesired cracking and coking leading to significant catalyst deactivation. In contrast, the use of non-acidic α-alumina and NaY zeolite may be valuable given the potential minimization of unwanted secondary reactions.

Regarding the various candidates VO_x supported catalysts for *n*-butane dehydrogenation, both redox and acid–base properties are studied here. Characterization of these catalysts is carried out using temperature programmed reduction and oxidation (TPR and TPO) and ammonia temperature programmed desorption (NH_3-TPD).

* Corresponding author. Tel.: +54-291-4861700; fax: +54-291-4861600.
E-mail address: mvolpe@plapiqui.edu.ar (M. Volpe).

0926-860X/$ – see front matter © 2004 Elsevier B.V. All rights reserved.
doi:10.1016/j.apcata.2004.05.017

2. Experimental

2.1. Catalyst preparation

A number of VO_x catalysts were considered in the present study as follows: γ-Al_2O_3 (Rhône Poulenc, 120 m^2/g), α-Al_2O_3 (Rhône Poulenc, 13 m^2/g), USY (TOSOH 320HOA, ultra stable Y zeolite, 3.5% Na and 626 m^2/g) and NaY (Strem Chemicals PRODUCT #: 14-8960, 731 m^2/g).

Before preparing the supported vanadium catalysts, the particles of support were calcined at 500 °C for 4 h under a GC quality air flow. Following this, approximately 2 g of support were contacted with $V(AcAc)_3$ (vanadium III acetylacetonate) solutions (Aldrich, 99.998% pure) in toluene.

The support impregnation was performed at room temperature for a 24 h period. The impregnated particles were filtered and separated from the supernatant liquid and the resulting cake was washed three times with fresh solvent. The resulting cake was dried first at 150 °C and following this, the impregnated particles (catalyst precursor) were calcined under a GC quality air stream at 600 °C for a 6 h period.

The same preparation methodology was consistently adopted while impregnating the various supports and this led to VO_x supported on USY, NaY, γ-Al_2O_3 and α-Al_2O_3. For the purpose of identifying the several VO_x supported catalysts the following codes are adopted in the upcoming sections: VO_x/USY (VO_x supported on USY), VO_x/NaY (VO_x supported on NaY), VO_x/γ-Al_2O_3 (VO_x supported on γ-Al_2O_3) and VO_x/α-$Al_2O_{3(}VO_x$ supported on α-Al_2O_3).

In addition to preparing an additional sample of VO_x supported on α-$Al_2O_{3,}$ a slightly different method was adopted. The alumina support was contacted with a pH 4 NH_4VO_3 (ammonium metavanadate) aqueous solution at room temperature for 24 h. Samples were subsequently filtered and calcined under air flow at 500 °C for 4 h. This sample is referred, in the present study as VO_xM/α-Al_2O_3.

Once the various catalyst samples prepared, the bulk amount of vanadium in each one of the catalysts was determined using atomic absorption spectroscopy.

2.2. Samples characterization

2.2.1. N_2 and Ar Isotherms

Nitrogen and argon adsorption were carried out at 77 K on an ASAP 2010 automatic adsorption analyzer equipped with micropore option (from 7Micromeritics). Before the measurements, samples weighing from 0.1 to 0.3 g were degassed at 100 °C for 1 h and at 300 °C for 10 h. Adsorption isotherms were measured in the $\sim 10^{-6}$ to 1, relative pressure range.

2.2.2. Temperature programmed reduction and oxidation

Both TPO and TPR experiments over fresh samples were conducted using an AutoChem II instrument.

A reducing gas mixture (10.2% H_2–89.8% Ar) was allowed to contact the catalyst sample at a 50 ml STP/min. Temperature was increased at 10 °C/min up to a maximum of 900 °C. Hydrogen concentration changes were determined in the outlet gas stream via a TCD detector. The area of the resulting peaks was integrated numerically, yielding the total hydrogen uptake volume.

TPO experiments were subsequently carried out employing the same method as for TPR analysis with samples being pretreated at 500 °C for 1 h under a 50 ml STP/min inert gas flow. Following this, samples were contacted with 5% O_2–95% He gas mixture. TPOs were effected for both VO_x/USY and VO_x/γ-Al_2O_3 after 40 or 80 min of having the catalyst sample under reducing conditions. TPO experiments also allowed estimating the coke deposited on aged catalysts. In these cases a 100 mg catalyst sample was employed.

2.2.3. Temperature programmed desorption

An AutoChem II analyzer from Micromeritics was used for TPD analysis. The catalyst sample (ranging 0.1–0.3 g), set in a quartz container, was degassed for 2 h at 500 °C. The sample was brought to saturation level using an NH_3/He gas mixture (4.55% ammonia, 95.55% helium). The adsorption of ammonia was carried out for 1 h at 140 °C. The ammonia flow was then switched off, and replaced by an inert purge gas (He) at a 50 ml STP/min rate for 1 h at the same temperature of ammonia adsorption. Then, the temperature was raised using a 15 °C/min ramp. As the temperature increased, desorption took place with the TCD signal being recorded.

2.3. Activity measurements

Catalytic activity tests were performed in a fixed bed micro-reactor with a mass of catalyst in the 0.07–0.25 g range. The weight of the catalyst sample was selected to keep in all cases a close to constant amount of vanadium, set at 4 mg.

The catalytic test was initiated with the catalyst sample being preheated using a 5 °C/min ramp under airflow until the 520 °C reaction temperature was reached. This preconditioning of the catalysts secured that the supported VO_x was under the fully oxidized state.

Following this, the true catalytic test was initiated feeding to the microreactor a 30 ml STP/min 10% of *n*-butane in nitrogen mixture. The outlet reactor products were GC analyzed periodically (every 4 min for a 1 h period), using a TCD detector and a Chromwas packed column.

On the basis of the data obtained the overall *n*-butane conversion and selectivity towards butenes formation were calculated.

3. Results

3.1. Catalysts bulk composition

Vanadium content for the various prepared catalysts is reported in Table 1. It can be observed that for both the NaY and α-Al_2O_3 supports, a small amount of vanadium was in-

Table 1
Physicochemical properties of VO_x/support catalysts

Sample	V (%)	BET catalyst (m^2/g)	BET support (m^2/g)	θ (%)[a]
VO_x/α-Al_2O_3	0.4	13	13	60
VO_xM/α-Al_2O_3	2.1	13	13	In excess to 100
VO_x/γ-Al_2O_3	2.2	80	80	55
VO_x/NaY	0.3	731	731	1
VO_x/USY	6.3	225	626	10

[a] Calculated assuming a unit area ($VO_{2.5}$) of 0.165 nm^2.

corporated into the supports with this being probably due to the very low OH concentration on the support surface. It was also noticed that the amount of supported V on α-Al_2O_3 increased for the sample prepared via the NH_4VO_3 precursor.

3.2. Catalysts characterization

3.2.1. BET area measurements

BET areas of the bare supports and those of the corresponding VO_x/support samples are reported in Table 1. It was noticed that the specific surface area of the support was unaffected upon the introduction of VO_x for both γ and α alumina. In contrast with this, a strong decrease of the specific surface area was observed for the USY supported catalyst, with the BET area being reduced by nearly 50% after vanadium impregnation. Considering the large size of the $V(AcAc)_3$ molecule, in the 50 Å range, it can be speculated that the VO_x/USY impregnation via the acetylacetonate molecule incorporation into the zeolite cage is largely unsuccessful with the VO_x species precursor essentially dispersed on the zeolite extra framework surface.

In this respect, it is important to mention that, vanadium oxides are known fluid catalytic cracking (FCC) catalysts poisons, with vanadium oxide species destroying the Brönsted acid sites and the structure of the ultrastable zeolite USY [7]. While, in the case of the catalysts of the present study, VO_x species are not exposed to steam, an important requirement for preventing the zeolite collapse. Although H_2O was formed during the initial calcination via combustion of the acetyl acetone, water was formed in minute amounts. On this basis it can be stated, that the prepared catalysts were in an essentially "free of steam/water atmosphere" during the preparation or pretreatment process. Thus there was no opportunity for the zeolite destruction to take place.

The theoretical coverage of the catalyst, θ, is calculated assuming a V_2O_5 unit cell area of 0.165 nm^2 in the (1 0 0) plane of vanadium pentoxide [8] and also considering the initial BET area of the support, as reported in Table 1. It can thus, be appreciated that a VO_x theoretical partial coverage of the supports is obtained for all the catalysts, except for VO_xM/α-Al_2O_3. In the latter case, the amount of VO_x exceeds the monolayer capacity of the support and this suggests the presence of V_2O_5 crystallites or a vanadia over layer on this catalyst sample.

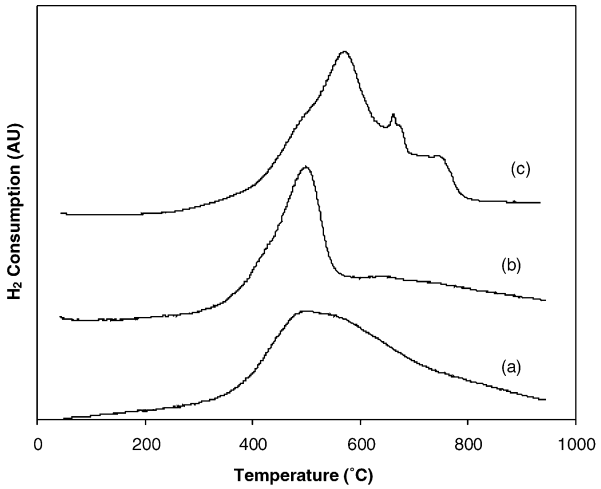

Fig. 1. TPR profiles for VO_x/support catalysts: (a) VO_xM/α-Al_2O_3; (b) VO_x/γ-Al_2O_3; (c) VO_x/USY.

3.2.2. Temperature programmed reduction

TPR is widely used to investigate the different types of oxidized species in vanadium oxides catalysts [9–12].

Fig. 1 reports the TPR profile for VO_x/γ-Al_2O_3 catalyst showing a main peak at 460 °C with a shoulder at 410 °C. This is consistent with the well-known strong affinity between alumina and vanadia [13]. As a result, monomeric or dimeric vanadates are formed at low vanadia loadings, with more prevalent polyvanadates chains at higher V-concentrations. Even more the higher vanadium concentrations may yield a supported monolayer [12,13]. Taking this into account, the H_2 consumption peak in the "b" profile of Fig. 1, corresponding to VO_x/γ-Al_2O_3 catalysts, is assigned to VO_x chains or bi-dimensional species reduction, while the lower temperature shoulder is postulated as the result of the reduction of mono or divandates species.

In the case of VO_xM/α-Al_2O_3 (profile "a" in Fig. 1) a broad H_2 consumption peak between 400 and 600 °C is observed. Since the V loading exceeds the monolayer capacity of the low surface α-Al_2O_3, it is expected that a V overlayer could grow on this support and that the consumption peak could be assigned to the reduction of those species.

Finally, the TPR profile of VO_x/USY (profile "c" in Fig. 1) displays distinctive trends of those corresponding to VO_x supported on α and γ-alumina. Three peaks were now noticed, with maximum temperature peaks placed at 580, 670 and 780 °C, respectively, and a shoulder at 460 °C. The 460 °C shoulder is attributed to the reduction of isolated VO_x species, while 580, 670 and 780 °C peaks are assigned to a three step crystalline V_2O_5 reduction [12].

In order to interpret these TPR profiles the following has to be considered: (a) a vanadia monolayer over USY is quite unlikely to be present, given the acid character of the zeolite support, (b) V−O−V bond formation is not viable and VO_x chains or a VO_x monolayer are not expected to develop.

Complementary XRD analyses were also effected to confirm the existence of crystalline V-oxide phases on the USY

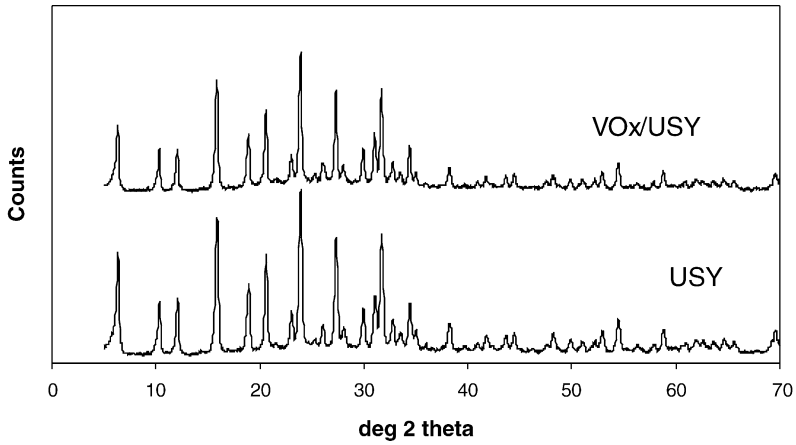

Fig. 2. XRD spectra for USY and VO_x/USY.

catalyst. These results are reported in Fig. 2. Unfortunately, the XRD failed to show VO_x modifications of the zeolite structure, and this given the vanadia crystallite sizes were below the minimum XRD detection limit. While only a minor decrease of the intensity of XRD peaks was observed, this change could not be positively assigned to a specific modification of the zeolite (extend of dehydration, reduction of zeolite concentration by the addition of vanadia species, slight framework dislocation/destruction).

3.2.3. TPO/TPR cycles

Catalysts undergo under the conditions of free of oxygen atmosphere dehydrogenation of *n*-butane rapid deactivation due to coke. Thus, it is necessary to restore catalyst activity with frequent catalyst regenerations. In this context, successive calcinations and TPR measurements were performed in order to evaluate the stability of the supported species.

Fig. 3 reports the TPR profiles for VO_x/γ-Al_2O_3 catalyst with no observable activity change through successive calcination–reduction cycles. These results show, that repeated calcination does not alter the reducibility of the supported V-species. In agreement with this, minor variations were observed in terms of the observable gas consumption for various TPRs.

On the other hand, the TPRs for the VO_x/USY catalyst show (Fig. 4) that this catalyst does undergo transformations through oxidation–reduction cycles. Fig. 4 shows that while the first two TPR were close, subsequent treatments display, in the high temperature range, quite different H_2 consumption patterns. Thus, it appears that the peaks as-

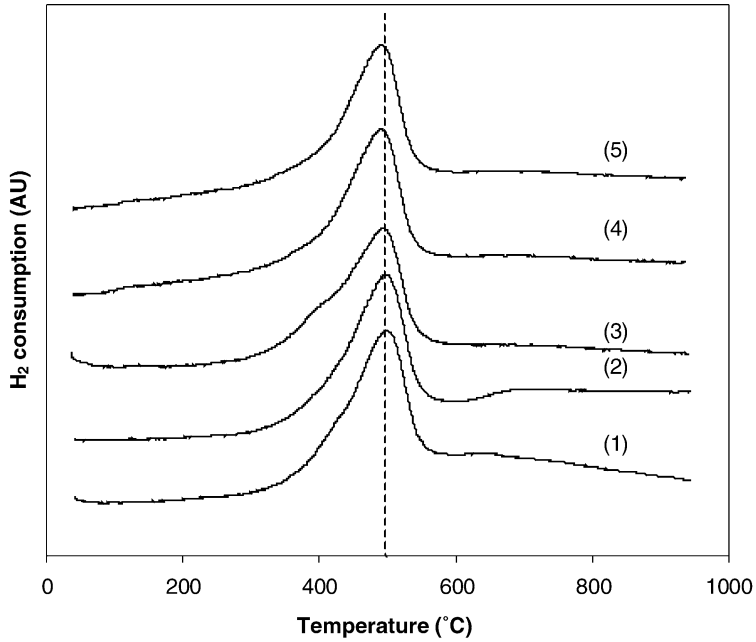

Fig. 3. Successive TPR profiles for VO_x/γ-Al_2O_3 catalyst. Pretreatment: calcination at 773 K. The number of each profile indicating to the number of calcination–reduction cycles performed over the sample.

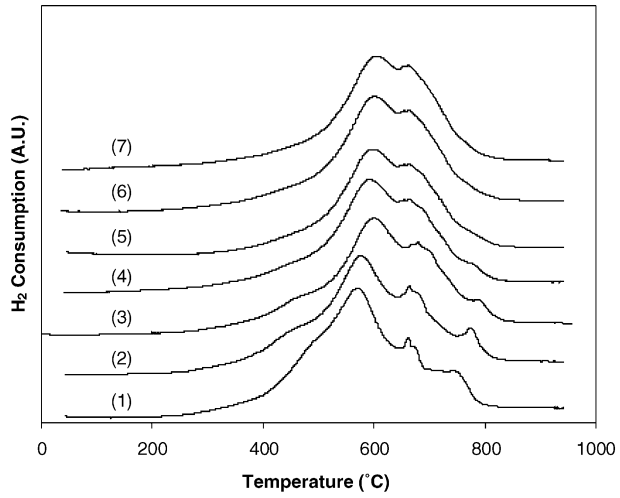

Fig. 4. Successive TPR profiles for VO_x/USY catalyst. Pretreatment: calcination at 773 K. The number assigned to each one of the TPR profiles refers to the number of calcination–reduction cycles performed over the sample.

signed to V_2O_5 crystallites become less defined, with the three-dimensional oxide species not being able to remain unaffected under regeneration conditions. Regarding hydrogen consumption patterns, as reported in Fig. 4, it is proven that the total H_2 consumption slightly diminishes from the first to the last experiment.

3.2.4. Temperature programmed desorption of NH_3

NH_3 TPD is frequently used to characterize the strength as well as the acid site amount on a solid surface. Due to its strong acidity and small molecular dimensions (3.70 Å × 3.99 Å × 3.11 Å) [14] ammonia is a suitable probe molecule for all OH groups on zeolite, even those accessible through pores, channels, or windows ≥ 4 Å. Fig. 5 reports the ammonia TPD for some of the catalysts used in this work. Besides, Table 2 gives the total amount of NH_3 desorbed in each case and the temperature corresponding to the maximum desorption peak (T_{max}).

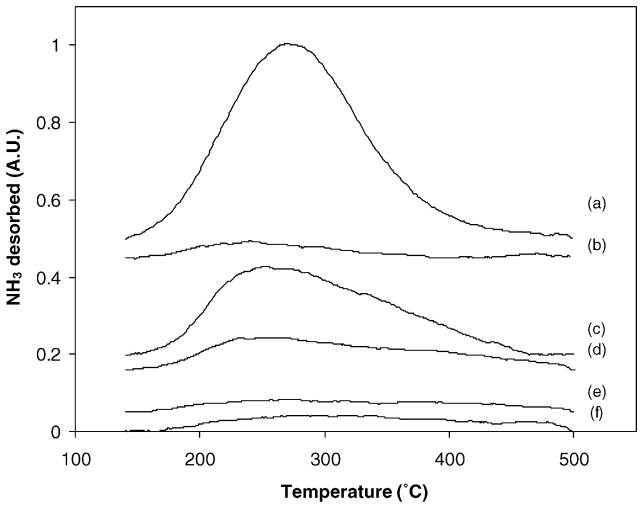

Fig. 5. Thermal desorption chromatograms of ammonia adsorbed at 140 °C for: (a) USY; (b) VO_x/USY; (c) γ-alumina; (d) VO_x/γ-Al_2O_3; (e) α-alumina; (f) VO_xM/α-Al_2O_3.

Table 2
Acidic properties of supports and the corresponding VO_x catalysts determined by NH_3 TPD

Sample	Ammonia desorbed at 140 °C (mL NH_3/g of solid)	T_{max} (°C)
USY	14.85	271
α-Al_2O_3	0.48	269
γ-Al_2O_3	7.01	253
VO_x/γ-Al_2O_3	3.08	260
Vo_xM/α-Al_2O_3	2.17	280
VO_x/USY	1.19	240

T_{max}: maximum desorption temperature.

3.2.4.1. USY and VO_x/USY. The USY zeolite sample displayed one single peak at 271 °C. This peak was assigned to both Brönsted and Lewis low-strength acid sites. Upon addition of VO_x on the USY support, the TPD peak strongly decreases (refer to profiles "a" and "b" in Fig. 5). While describing this effect it is important to consider that V loadings in the zeolite are quite low (6.3%). Considering the very large surface available in the USY support only partial surface coverage is achieved. Thus, it is possible to argue that the VO_x addition reduces the acidity of the zeolite and this is likely to be due to the V_2O_5 crystallite phase formation, which blocks zeolite windows and supercages and strongly hinders NH_3 accessibility. It is perhaps possible that in a situation like the one described, the NH_3 only measures the external surface and/or cracks surfaces of the USY.

Another interesting observation relates to the shifting of TPD peak from 271 to 240 °C for USY and VO_x/USY, respectively. It is very likely this shift is the result of the VO_x own acidity, with the acidity measured via TPD being the combined contribution of the support and of VO_x species.

3.2.4.2. γ-Al_2O_3 and VO_x/γ-Al_2O_3. Concerning TPD acidity in γ-Al_2O_3, profile "c" in Fig. 5, a 253 °C peak was observed with this peak being assigned to the support acidity. It can be noticed comparing this TPD profile with the one corresponding to VO_x/γ-Al_2O_3 that the acid site concentration decreases considerably after adding the VO_x to the support (refer "d" profile). This acidity reduction may be attributed to the coverage of the surface of the γ-alumina with VO_x species. However, since the support coverage is partially accomplished (refer to Table 1, last column) a certain number of acid sites remain vacant after VO_x addition.

3.2.4.3. α-Al_2O_3 and VO_xM/α-Al_2O_3. A minor desorption peak was observed in the TPD profile of α-Al_2O_3, a non-acid solid. Surprisingly, the acidity increased for the VO_xM/α-Al_2O_3. It appears, in this respect, that the supported VO_x monolayer also contributes with its own acidity.

3.3. Catalytic activity

Catalytic runs were preceded with a number of blank runs. During these blank runs, the support only was loaded in the reactor. No measurable *n*-butane conversion was observed at the catalytic reaction conditions, for both α-Al_2O_3 or γ-Al_2O_3. This proves two important facts: (a) the alumina support is inert under reaction conditions; (b) there is no contribution of the homogeneous *n*-butane conversion. Furthermore blank tests with USY gave low 1–3% *n*-butane conversions proving again the lack of contribution of the support as well as the negligible homogenous conversion of *n*-butane.

Concerning the catalytic activity experiments, *n*-butane conversions on VO_x/USY, VO_x/γ-Al_2O_3 and VO_xM/α-Al_2O_3 catalysts are reported in Fig. 6. Data corresponding to VO_x/α-Al_2O_3 and VO_x/NaY are not reported in Fig. 6 or reviewed in this section given the negligible catalytic activity observed for these two catalysts.

At 520 °C and with a *n*-butane/nitrogen feed of 1:9 mol/mol, the allowed thermodynamic *n*-butane conversion to 1-butene, *cis* and *trans* 2-butene, and 1,3-butadiene, is 65%. It should in this respect be noted that the experimentally observed *n*-butane conversion for both VO_x/USY and VO_x/γ-Al_2O_3 was considerably lower than the thermodynamic upper conversion limit.

Regarding the reaction experiments, as reported in Fig. 6, one can observe a starting reaction phase where *n*-butane conversion increases with time-on-stream. This consistent result obtained for both VO_x/γ-Al_2O_3 and VO_x/USY yielded, respectively, at 4 min, maxima of 9 and 11% *n*-butane conversions. Thus, it appears that the *n*-butane dehydrogenation, under a free of oxygen atmosphere, proceeds via an initiation phase with the formation of key intermediate species or active site that plays an important role later in the subsequent reaction steps.

Following this initial phase, with *n*-butane conversion reaching a maximum level, *n*-butane conversion starts decreasing with VO_x/γ-Al_2O_3 becoming fully inactive and VO_x/USY stabilizing in a low activity level at 40 min of time-on-stream.

Harlin et al. [6] measured *n*-butane conversion at 580 °C and WHVS of $5\,h^{-1}$over VO_x supported on calcined alumina. These authors also observed a slight increase in conversion from 18 to 23% during the first 5 min of time-on-stream and this was in agreement with the findings of this study showing an initial reaction period of increased catalytic activity.

In Fig. 6 it can also be noticed that the VO_x/USY remains for all the time-on-stream studied more active than VO_x/γ-Al_2O_3. Even though cracking reactions, promote coke formation; the VO_x/USY catalyst still remains, after 40 min, catalytically active. It thus appears as if the surface in this catalyst is subjected, after a given time-on-stream, to a much slower activity losses, still displaying under these conditions a favorable performance towards the reactions leading to olefin formation.

The VO_xM/α-Al_2O_3 displayed however, a very limited *n*-butane conversion, even though a relatively high concentration of VO_x species is present on this catalyst, and its acidity is higher than the acidity of the VO_x/USY (refer to Table 2). This behavior can be assigned to the formation of a vanadia overlayer on the α-Al_2O_3 support with the expected result of a low fraction of V-species exposed, leading overall to a low concentration of V-active sites.

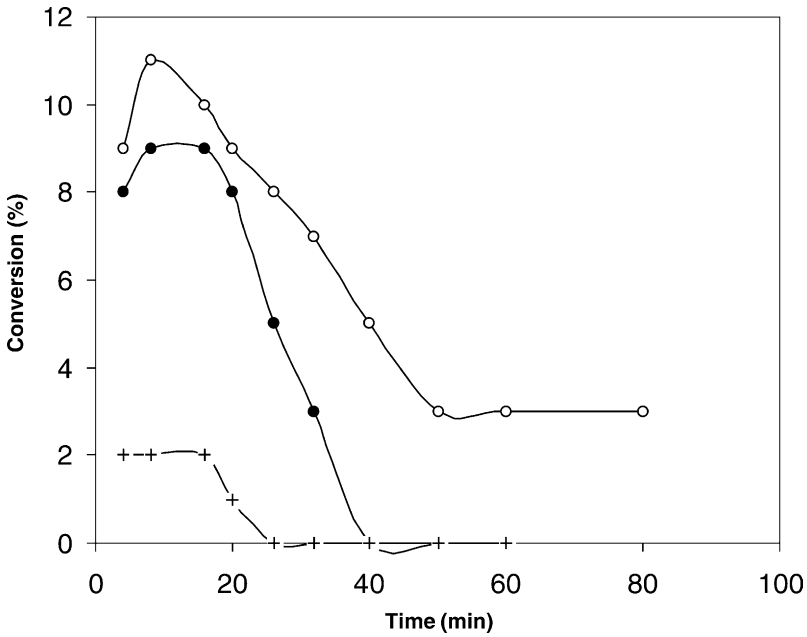

Fig. 6. *n*-Butane conversion at 520 °C with calcined VO_x/support catalysts. References: (○) VO_x/γ-Al_2O_3; (●) VO_x/USY; (+) VO_xM/α-Al_2O_3.

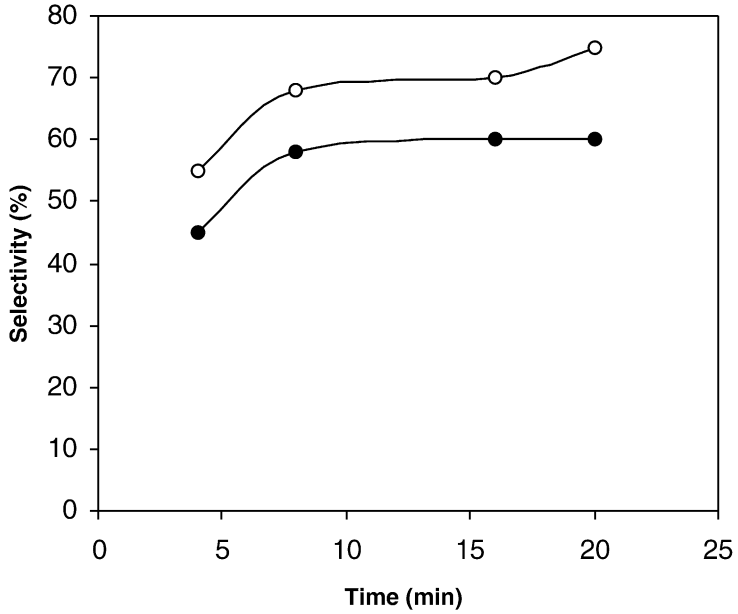

Fig. 7. Butenes selectivity at 520 °C with calcined VO_x/support catalysts. References: (●) VO_x/γ-Al_2O_3; (○)VO_x/USY.

Finally, if one envision this reactor as a continuous circulating fluidized bed reactor the data of this study allows to predict that one should remove the successfully prepared catalyst (e.g. VO_x/USY) every 30 min of catalyst residence time and this to achieve a good level of overall activity. Following this the catalyst should be fully reoxidized and sent back again for another catalytic dehydrogenation cycle.

Concerning reaction products the following species were consistently observed during the catalytic activity tests: CO_x, 1-butene, 2-*trans* and 2-*cis* butene, 1,3-butadiene, and small amounts of methane, propane and *i*-butane. The formation of coke was also detected in the spent catalysts (refer to Section 4). Given coke amounts were estimated to be, in all cases below 2% coke was not included in selectivity calculations. In addition no oxygenated products were detected thus no oxygenate species were needed to be accounted in the selectivity analysis.

The dependence of alkene selectivity, *S*%, with catalyst time-on-stream is described in Fig. 7 and this for the most active catalysts: VO_x/USY and VO_x/γ-Al_2O_3. Product distribution is reported in Table 3 for a 4 min catalyst time-on-stream. Reviewing product distribution, it was also observed that product distribution was no constant and varied with catalyst time-on-stream. In addition it was also observed that the selectivity pattern was very specific for each one of the catalysts studied. No selectivity results corresponding to VO_xM/α-Al_2O_3 are reported and this given the uncertainty of defining selectivity at low conversions.

Table 3
Distribution of products at 4 min of reaction for the dehydrogenation of *n*-butane with calcined VO_x/USY and VO_x/γ-Al_2O_3

Catalyst	*S*%, 4 min[a]	*S*%, CO_x 4 min[b]	*S*%, other prod[c]	O_2 consumed[d]
VO_x/γ-Al_2O_3	45	30	25	140
VO_x/USY	56	31	13	70

[a] Selectivity to butenes.
[b] Selectivity to CO_x.
[c] Selectivity to other products (propane, methane, isobutane).
[d] ml/g of V measured in TPO experiments.

The %S increased consistently (refer to Fig. 7) for both the VO_x/USY, from 55 to 75% and for the VO_x/γ-Al_2O_3, from 45 to 60%. An interesting result was that butenes selectivity of the VO_x/USY catalyst surpassed in all cases those for VO_x/γ-Al_2O_3. These differences in the butene selectivity were ascribed to the acidity differences between these two catalysts, a dominant property determining butane dehydrogenation into butenes.

Another consistent and valuable observation both for VO_x/γ-Al_2O_3 and for VO_x/USY, was given by the fact that CO_x formation was only noticeably at 4 min with no CO_x measurements afterwards. This early CO_x formation can be linked to the reduction of V^{5+} sites and this happens at the same time-on-stream than the maximum *n*-butane conversion is observed (Fig. 6). Furthermore, this free of CO_x product species, for times-on-stream larger than 4 min was very encouraging, given it allows to argue that two of the catalysts developed in this study display a high selective for *n*-butane conversion, yielding valuable non-CO_x products only.

Table 3 reports the fractions of other than butenes and CO_x product species formed via cracking and isomerization reactions (propane, methane, isobutane). Selectivity towards these species is higher for VO_x/γ-Al_2O_3 than for VO_x/USY, during the first 4 min.

3.3.1. Activity of regenerated sample

Due mainly to the coke formation, samples become inactive with time-on-stream. Thus, it is important to estab-

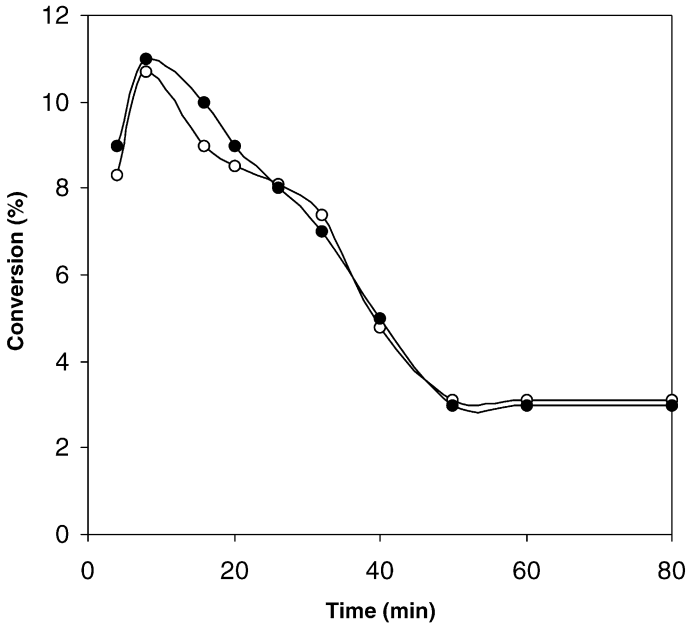

Fig. 8. *n*-Butane conversion at 520 °C with fresh and regenerated VO_x/USY catalysts. References: (●) fresh VO_x/USY; (○) regenerated VO_x/USY.

lish if a regeneration treatment recovers aged sample activity. In this context, the dehydrogenation reaction was carried out over used $VO_x/\gamma\text{-}Al_2O_3$ and VO_x/USY catalysts. The aged samples were calcined in situ for 1 h at the reaction temperature and subsequently a new catalytic test was carried out. Once again, the activity and selectivity were measured at the same conditions as for fresh samples. The dependence of *n*-butane conversion with time-on-stream for a regenerated VO_x/USY sample is reported in Fig. 8. For the sake of comparison the data corresponding to a fresh VO_x/USY sample are also reported. Both catalyst tested, displayed an activity-selectivity behavior with time-on-stream very close to the one for the fresh catalyst indicating that the catalyst deactivation by coke can be completely reversed and that the nature of VO_x species was the same following reaction-regeneration treatments.

3.4. Temperature programmed oxidation

TPO tests were carried out for $VO_x/\gamma\text{-}Al_2O_3$ and VO_x/USY fresh and spent catalysts only and this to determine the amounts of coke formed during the reaction period (gray lines in Fig. 9). The gray TPO curves show a broad negative peak, assigned to the formation of CO_2 resulting from coke oxidation.

In both cases, the coke was calcined at the close temperatures, suggesting that the nature of coke species was, for both catalysts, similar. Even more given that calcinations were effected under oxygen excess conditions, it was assumed that combustion was complete and the TCD signals were directly proportional to the CO_2 formed and thus to the coke present on the catalyst surface.

On this basis the CO_x amount evolved per gram of vanadium (reported in Table 3) was calculated. It was observed that this amount was much higher (approximately twice) for $VO_x/\gamma\text{-}Al_2O_3$ than for VO_x/USY. These findings show higher coke levels on the $VO_x/\gamma\text{-}Al_2O_3$ catalyst and are in agreement with the catalytic test results, which indicate that cracking reactions and catalyst decay are more dominant over $VO_x/\gamma\text{-}Al_2O_3$ than over VO_x/USY.

Furthermore, the TPO profiles in the subsequent second oxidation cycle (black lines in Fig. 9) showed a main peak, with these positive peaks representing O_2 consumption of an 5% O_2/95% He mixture. A maximum peak at 130 °C was observed for $VO_x/\gamma\text{-}Al_2O_3$. This early peak was assigned

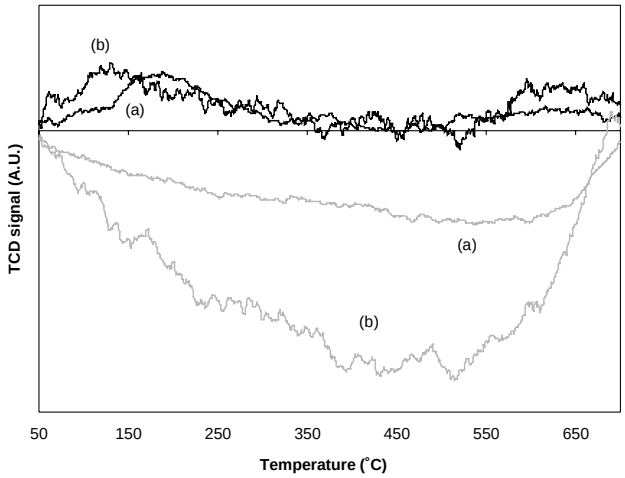

Fig. 9. TPO profiles. Gray curves refer to the TPO carried out after the catalysts were used in a complete *n*-butane dehydrogenation cycle lasting 40 (curve b) for $VO_x/\gamma\text{-}Al_2O_3$ and 80 min (curve b) for VO_x/USY.

to the VO_{x-1} species re-oxidation. For the VO_x/USY there were however, two extra peaks centered at 190 and 450 °C, respectively. The first one was similar to the one observed for vanadium on alumina, while the peak at the higher temperature was assigned to the oxidation of partially reduced vanadia crystallites. Thus, TPO profiles were, in this respect well in agreement with TPR curves and pointed towards the presence of V_2O_5 crystallites on VO_x/USY catalysts.

4. Discussion

Based on the reported results, it can be mentioned that the *n*-butane catalytic dehydrogenation in a free of oxygen atmosphere, both in terms of activity and selectivity is related to the various catalyst surface properties as described via the several characterization tests performed.

In this respect, it was observed that the nature of the support, be this USY or γ-alumina, leads to different vanadium species, well dispersed mono or dimeric vanadates, VO_x chains, vanadia overlayer or V_2O_5 crystallites.

The vanadium pentoxide crystallites formed are specific species of the VO_x/USY catalyst, and this leads to a number of effects such as blocking of windows and supercages, reduction of specific surface area and TPD acidity modifications. The V_2O_5 crystallites appear to limit considerably isomerization and cracking reactions favoring coke formation. Besides, well-dispersed VO_x species, also present in the VO_x/USY catalyst, promote the formation of butenes, turning the VO_x/USY in the most active and selective catalysts for the *n*-butane catalytic dehydrogenation.

Concerning the VO_x/γ-Al_2O_3 catalyst, TPR results show highly dispersed vanadia on the alumina surface, with no evidence of V_2O_5 crystallites formation.

Furthermore, VO_x addition appears to reduce support acidity, as observed via ammonia TPD, yielding as a result slightly acidic catalysts, with this mild acidity being critical to the formation of active sites. Even more, given the relatively high catalytic dehydrogenation activity observed a high concentration of VO_x exposed active sites can be hypothesized.

It also appears in the catalytic dehydrogenation of butane there are significant mechanistic changes occurring during the first minutes of catalyst time-on-stream. During this initial phase either the nature or the controlling reaction step changes with VO_x forming some CO_x. Once this initial period completed no additional formation of CO_x is noticed with all observed products being hydrocarbon species. Since the *n*-butane conversion increases during the first few minutes of reaction, one could envisage that a pre-reduction prior to catalyst exposure to *n*-butane (a common treatment for both Pt and Cr_2O_3 supported on alumina catalyst) could as well increase the initial conversion. Supporting this view it can be stated that in separate catalytic runs performed by our group over prereduced VO_x/γ-Al_2O_3 under H_2 flow at 520 °C, and this led at 4 min to higher *n*-butane conversions than while using calcined catalysts. Furthermore, under those conditions no CO_x was detected. However, no reproducible data was obtained over prereduced VO_x/USY, and the effect of pre-reduction on catalyst performance, is considered to be a substantial issue, left for a forthcoming study.

Finally, regarding to VO_xM/α-Al_2O_3 catalyst, the selected catalyst preparation leads to an essentially inactive material. It is hypothesized, on the basis of TPR data, that there is a vanadium overlayer formed which strongly contribute to the low activity of this catalyst.

Results of the present study also point towards the significance of moderating, as much as possible, the butane and butenes catalytic cracking activity of the prepared catalysts. Cracking reactions are promoted on the acid sites of the bare support with selectivity towards the desired olefin products being negatively affected. Thus, catalytic cracking activity should be restricted, as much as possible, using weak acidity supports with all this leading to a minimization of undesirable cracking reactions.

As a result and from the scenario depicted above, it can be suggested that the best butane dehydrogenation catalyst in oxygen free atmosphere should be one designed, as is the case of the VO_x/USY, with a highly dispersed reduced VO_x phase on a slightly acidic support.

5. Conclusions

The following are the relevant conclusion of the present study:

- Several VO_x catalysts supported on different oxide carriers were successfully prepared.
- VO_x/USY and VO_x/γ-Al_2O_3 catalysts prepared via impregnation with $V(AcAc)_3$ precursors, dried and calcined, led to active and selective materials for *n*-butane dehydrogenation under a free oxygen atmosphere.
- The VO_x/USY catalysts provided a high 60–75% alkene selectivity. This selectivity, was higher than the one for the VO_x/γ-Al_2O_3, with this selectivity difference being assigned to the mild VO_x/USY acidity.

Acknowledgements

This work was supported with funding from the Universidad Nacional del Sur, the Consejo Nacional de Investigaciones Científicas y Técnicas (CONICET) and Natural Sciences and Research Council of Canada (NSRCC).

References

[1] B.M. Weckhuysen, R.A. Schoonheydt, Catal. Today 51 (1999) 223.
[2] C. Larese, J.M. Campos-Martin, J.L.G. Fierro, Langmuir 16 (2000) 10294.

[3] A. Pantazidis, S.A. Bucholz, H.W. Zanthoff, Y. Shcurman, C. Mirodatos, Catal. Today 40 (1998) 207.
[4] D. Creaser, B. Andersson, R.R. Hudgins, P.L. Silveston, J. Catal. 182 (1999) 264.
[5] M.E. Harlin, V.M. Niemi, A.O.I. Krause, J. Catal. 195 (2000) 67.
[6] M.E. Harlin, V.M. Niemi, A.O.I. Krause, B.M. Weckhuysen, J. Catal. 203 (2001) 242.
[7] C. Trujillo, U. Navarro Uribe, P. Knops-Gerrits, L. Oviedo, P. Jacobsz, J. Catal. 168 (1997) 1.
[8] J. Eon, R. Olier, J.C. Volta, J. Catal. 145 (1994) 318.
[9] L. Roozeboom, J. Van Hengstum, G. Van Ommen, H. Bosch, P. Gellings, in: Proceedings of the Eighth International Congress of Catalysis, vol. 4, Dechema, Frankfurt-am Main, 1984, p. 297.
[10] M. Koranne, J. Goodwin, G. Marcelin, J. Catal. 148 (1994) 369.
[11] M. Ferreira, M. Volpe, J. Mol. Catal. A 184 (2002) 349.
[12] H. Bosch, B.J. Kip, J.G. van Ommen, P. Gellings, J. Chem. Soc., Faraday Trans. 80 (1984) 2479.
[13] I.E. Wachs, B. Weckhuysen, Appl. Catal. A. G157 (1997) 67.
[14] C. Webster, R. Drago, M. Zerner, J. Am. Chem. Soc. 120 (1998) 5509.